Journal of Computational Physics **175,** 24–49 (2002)
doi:10.1006/jcph.2001.6878, available online at http://www.idealibrary.com on IDEAL®

Application of the Difference Gaussian Rules to Solution of Hyperbolic Problems

II. Global Expansion

Sergey Asvadurov,* Vladimir Druskin,* and Leonid Knizhnerman†

**Schlumberger-Doll Research, Old Quarry Road, Ridgefield, Connecticut 06877-4108; and †Central Geophysical Expedition, Narodnogo Opolcheniya St., 40-3, Moscow 123298, Russia*
E-mail: asvadurov@slb.com; druskin@slb.com; mmd@cge.ru

Received February 2, 2001; revised June 26, 2001

This work is the sequel to S. Asvadurov *et al.* (2000, *J. Comput. Phys.* **158,** 116), where we considered a grid refinement approach for second-order finite-difference time domain schemes. This approach permits one to compute solutions of certain wave equations with exponential superconvergence. An algorithm was presented that generates a special sequence of grid steps, called "optimal," such that a standard finite-difference discretization that uses this grid produces an accurate approximation to the Neumann-to-Dirichlet map. It was demonstrated that the application of this approach to some problems in, e.g., elastodynamics results in a computational cost that is an order of magnitude lower than that of the standard scheme with equally spaced gridnodes, which produces the same accuracy. The main drawback of the presented approach was that the accurate solution could be obtained only at some a priori selected points (receivers). Here we present an algorithm that, given a solution on the coarse "optimal" grid, accurately reconstructs the solution of the corresponding fine equidistant grid with steps that are approximately equal to the minimal step of the optimal (strongly nonuniform) grid. This "expansion" algorithm is based on postprocessing of the approximate solution, is local in time (but not in space), and has a cost comparable to that of the discrete Fourier transform. An approximate inverse to the "expansion" procedure—the "reduction" algorithm—is also presented. We show different applications of the developed procedures, including refinement of a nonmatching grid. Numerical examples for scalar wave propagation and 2.5D cylindrical elasticity are presented.

Key Words: finite differences; Gaussian rules; exponential convergence; hyperbolic problems; linear elasticity; wave propagation.

0021-9991/02 $35.00

1. INTRODUCTION

Recently an algorithm was presented for constructing a special sequence of steps which permits one to compute Neumann-to-Dirichlet maps of certain Helmholtz equations with exponential super-convergence [2]–[7]. The algorithm is based on Padé–Chebyshev approximation of the impedance on a predefined spectral interval, and the resulting "optimal" steps were successfully applied to solutions of problems in elastodynamics and electromagnetics. This grid optimization approach allows one to obtain spectral convergence of the Green function at a subset of a priori prescribed points (receivers) using second-order finite-difference time domain (FDTD) schemes with between two and four grid points per wavelength, though globally the new scheme converges not faster than the standard equidistant second-order scheme. The refinement of the optimal grid had to be done at all the receivers as well as at the source points. For some applications in remote sensing, where the solution is generated by few point sources and measured at only few receiver points, it is not a disability, but generally it is an essential drawback.

One can view the grid optimization procedure as an extension of Gaussian quadrature to second-order finite-difference schemes. Just as a Gaussian k-point quadrature rule for numerical integration is chosen to be exact for $2k$ polynomials, we choose our k-node grid so that some $2k$ functionals of the solution are exact. It so happens that these functionals are related to projections of the exact solution on certain subspaces with good (spectral) approximation properties. In other words, in some sense, three-point FD approximations with "optimal" steps are equivalent to spectral Galerkin approximations, and the latter can be eventually recovered from the former using a linear postprocessing transformation [8]. Theoretically, this procedure should yield global exponential convergence, but we found it difficult to implement, mainly due to some loss of accuracy.

Here we simplify, and eventually circumvent, this problem by approximating a FD operator on a fine equidistant grid, instead of the differential operator, as was done originally. We use the Padé–Chebyshev approximation of the finite-difference impedance, computed on a fine grid, instead of the true impedance of the continuous problem. As a result, for a given spectral interval we can approximate with computer precision the accurate impedance of the fine equidistant finite-difference scheme by the impedance of the coarse optimal scheme (with much fewer grid nodes). The steps of the optimal grid turn out to be increasing, with the first, minimal, step being approximately equal to the step of the fine equidistant grid. The grid optimization algorithm can now be viewed as a *grid reduction*.

The grid *expansion* algorithm presented here transforms the solution from the coarse optimal grid to the fine equidistant one. Let $\mathbf{u}_k(\psi) = [u_k(x_1, \psi), \ldots, u_k(x_k, \psi)]^T$ be the FD solution of a multidimensional problem obtained on the optimal grid $x_1, \ldots, x_k$, and let $\mathbf{u}_N(\psi) = [u_N(\tilde{x}_1, \psi), \ldots, u_N(\tilde{x}_N, \psi)]^T$ be the solution on the equidistant grid $\tilde{x}_1, \ldots, \tilde{x}_N$, with $N \gg k$ (in both cases the dependence on other spatial and/or temporal variables is hidden in the dependence on vector ψ). Here we assume that $x_1 = \tilde{x}_1$ and that the equation is homogeneous with a nonhomogeneous boundary condition at this node. The optimal grid exactly matches the impedance of the equidistant grid at the first node for some $2k$ fine grid solutions. The Padé–Chebyshev approximant used for the match converges at least exponentially, while the equidistant finite-difference scheme converges only with the second order, which is why with relatively small k (compared to N) the optimal grid would match the impedance of smooth enough fine grid solutions with error that is smaller than the error of approximation of (either) grid impedance to the true continuous impedance. In

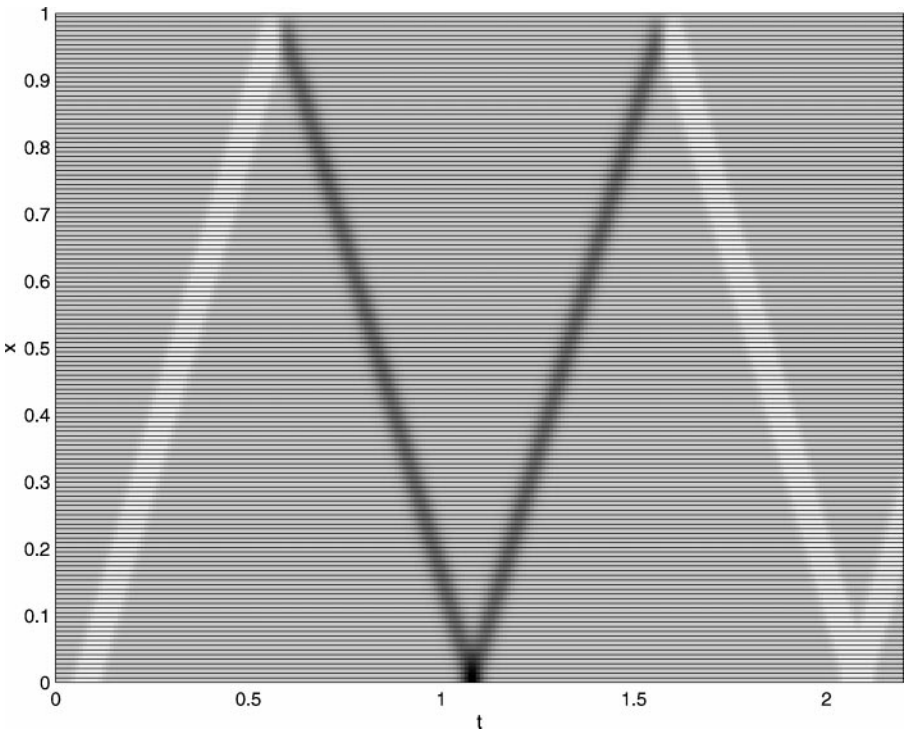

FIG. 1. Propagation of a scalar 1D wave on the equidistant mesh.

other words, the fine equidistant grid solutions can be well approximated on a relatively small subspace. For this subspace the expansion algorithm is defined as

$$\mathbf{u}_N(\psi) = S\mathbf{u}_k(\psi), \tag{1.1}$$

where S is an $N \times k$ (full) matrix such that $S\mathbf{e}_{k,1} = \mathbf{e}_{N,1.}$ To achieve accuracy of 1% on the equidistant grid for wave problems, it is typically required to have more than 20 points per wavelength, while the expansion algorithm reconstructs such fine grid solutions with good precision using no more than 3–4 points per wavelength on average. We should notice that except for the first node the optimal solution and the fine equidistant one do not match exactly even for accidentally coinciding nodes, and so expansion is not equivalent to interpolation. For inhomogeneous equations we also need to construct the inverse to this expansion transformation, what we call "reduction."

The main concept can be illustrated by Figs. 1 and 2, in which we show the propagation of a one-dimensional scalar wave. The problem is the same as in [2, Section 2.3]; it is given by the homogeneous 1D wave equation on $[0, 1] \times [0, T]$ with zero initial conditions, the homogeneous Dirichlet condition at $x = 1$, and the Neumann condition at $x = 0$ that defines the source term. Here ψ is equivalent to the time variable. The solution is a Gaussian wavelet, the results of its computation on the fine equidistant grid are presented in Fig. 1. The mesh[1] is also shown; here the total number of mesh points is 300. As we see, the wave packet remains compact at all time. In Fig. 2 one can see the solution, computed on a corresponding

[1] Every second mesh point is omitted in this figure because of the resolution limitation of the plotting software.

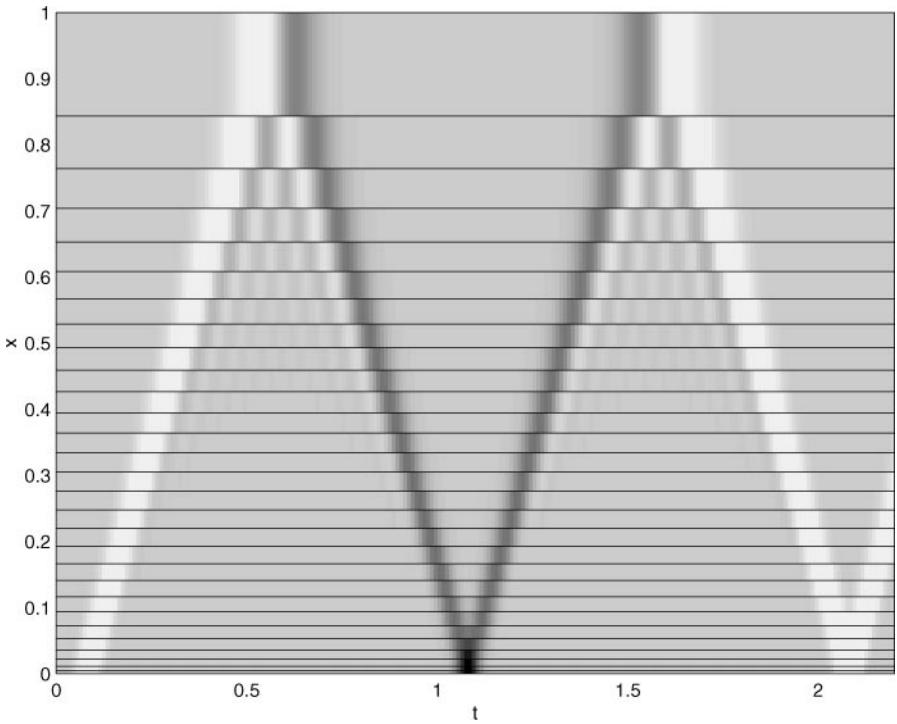

FIG. 2. Propagation of a scalar 1D wave on the optimal mesh corresponding to the equidistant mesh presented in Fig. 1.

optimal mesh. The mesh is also shown; its minimal step is approximately equal to the step of the equidistant grid, but the total number of mesh points here is 32. On this mesh, as the wave is traveling away from the point $x = 0$, definite dispersion appears, which dies away as the wave is propagating back to the origin, where optimal and fine equidistant solutions coincide with the precision of the calculation of the optimal mesh (usually the computer double precision). We obtain expansion matrix S that transforms the optimal solution to the fine equidistant one at all grid nodes of the equidistant grid and compare the error of this transformation to the error of the approximation of impedance.

It will be demonstrated that this technique can be easily applied to complicated multidomain problems. We will also consider different applications of the described procedures, including one to nonmatching grids, for which some subdomains are gridded in a standard equidistant fashion, while others employ the optimal mesh in the directions tangential to the interfaces. In this case the expansion and reduction transformations are used to match the solution at the interfaces at every time step of the FD experiment.

2. PRELIMINARIES

Consider a 1D wave equation on $[0, L] \times [0, T]$, written as a first-order system

$$\frac{d\hat{u}}{dt} = \frac{d\hat{v}}{dx}, \quad \frac{d\hat{v}}{dt} = \frac{d\hat{u}}{dx}, \tag{2.1}$$

with zero initial and some boundary conditions, which will be specified later. Using the Fourier transformation $u = \int \hat{u} e^{-iwt}\, dt$, $v = \int \hat{v} e^{-iwt}\, dt$, we reduce (2.1) to the first-order ordinary differential equation system

$$\sqrt{\lambda} u = \frac{dv}{dx}, \quad \sqrt{\lambda} v = \frac{du}{dx}, \tag{2.2}$$

where $\lambda = -\omega^2$. Throughout this paper we assume that u and v vanish for $\omega > \omega_{\max}$, i.e., we are looking for an approximation to the solution of (2.2) on the spectral interval $[\lambda_1, \lambda_2]$, where $\lambda_1 = -\omega_{\max}^2$ and $\lambda_2 = 0$.

2.1. The General 1D Scheme

We consider the discretization of the system (2.2) with the mixed boundary conditions $u(L) = 0$ and $u_x(0) = -1$,

$$\begin{aligned} \sqrt{\lambda} u_i &= \frac{v_i - v_{i-1}}{\hat{h}_i}, \quad i = 1, \ldots, k, \quad u_{k+1} = 0, \\ \sqrt{\lambda} v_i &= \frac{u_{i+1} - u_i}{h_i}, \quad i = 1, \ldots, k, \quad v_0 = -\frac{1}{\sqrt{\lambda}}. \end{aligned} \tag{2.3}$$

This can be rewritten in a matrix form as

$$\sqrt{\lambda}\mathbf{u} - X\mathbf{v} = \hat{h}_1^{-1}\mathbf{e}_1/\sqrt{\lambda}, \quad \sqrt{\lambda}\mathbf{v} - Y\mathbf{u} = 0, \tag{2.4}$$

where $\mathbf{u}$, $\mathbf{v}$ are vectors of length k, $\mathbf{u} = (u_1, \ldots, u_k)$, $\mathbf{v} = (v_1, \ldots, v_k)$, X is a matrix with $1/\hat{h}_i$ on the main diagonal and $-1/\hat{h}_i$ on the subdiagonal, and Y is a matrix with $-1/h_i$ on the diagonal and $1/h_i$ on the superdiagonal.

It is easily shown by direct computation that

$$(BX)^T = -CY, \tag{2.5}$$

where $B = \mathrm{diag}(\hat{h}_i)$ and $C = \mathrm{diag}(h_i)$.

System (2.4) is often written as a single equation for $\mathbf{u}$ as

$$\lambda\mathbf{u} - XY\mathbf{u} = \hat{h}_1^{-1}\mathbf{e}_1. \tag{2.6}$$

To bring this system to a symmetric form, we multiply it on the left by $B^{1/2}$, and let $\tilde{\mathbf{u}} = B^{1/2}\mathbf{u}$, which leads to

$$\lambda\tilde{\mathbf{u}} - H\tilde{\mathbf{u}} = \hat{h}_1^{-1/2}\mathbf{e}_1, \tag{2.7}$$

where $H = B^{1/2}XYB^{-1/2}$ is easily checked to be symmetric.

One could also write (2.4) as an equation for $\mathbf{v}$,

$$\lambda\mathbf{v} - YX\mathbf{v} = h_1^{-1}\hat{h}_1^{-1}\mathbf{e}_1/\sqrt{\lambda}, \tag{2.8}$$

or as a corresponding system for $\tilde{\mathbf{v}} = C^{1/2}\mathbf{v}$,

$$\lambda\tilde{\mathbf{v}} - H_{(d)}\tilde{\mathbf{v}} = \hat{h}_1^{-1}h_1^{-1/2}\mathbf{e}_1/\sqrt{\lambda}, \tag{2.9}$$

where $H_{(d)} = C^{1/2}YXC^{-1/2}$ is also symmetric. The subscript "d" here and in the future stands for "dual," since problem (2.9) is considered to be dual to problem (2.7).

Denote the eigenvalues of H by θ_i and the corresponding eigenvectors by $\tilde{\mathbf{s}}_i$, $\|\tilde{\mathbf{s}}_i\| = 1$, and note that $\theta_i \le 0$. In fact,

$$\begin{aligned}\theta_i = \langle \tilde{\mathbf{s}}_i, H\tilde{\mathbf{s}}_i\rangle &= \left\langle \tilde{\mathbf{s}}_i, B^{1/2}XYB^{-1/2}\tilde{\mathbf{s}}_i\right\rangle = \left\langle B^{-1/2}\tilde{\mathbf{s}}_i, BXYB^{-1/2}\tilde{\mathbf{s}}_i\right\rangle \\ &= -\left\langle C^{1/2}YB^{-1/2}\tilde{\mathbf{s}}_i, C^{1/2}YB^{-1/2}\tilde{\mathbf{s}}_i\right\rangle \le 0; \end{aligned} \tag{2.10}$$

here (2.5) was used, and the brackets denote the standard inner product.

LEMMA 2.1. *The eigenvalues of $H_{(d)}$ are θ_i, and its eigenvectors $\tilde{\mathbf{s}}_i^{(d)}$ are related to $\tilde{\mathbf{s}}_i$ by the following equalities*:

$$\tilde{\mathbf{s}}_i^{(d)} = \frac{1}{\sqrt{-\theta_i}} C^{1/2}YB^{-1/2}\tilde{\mathbf{s}}_i, \quad \|\tilde{\mathbf{s}}_i^{(d)}\| = 1, \tag{2.11}$$

$$\tilde{\mathbf{s}}_i = \frac{-1}{\sqrt{-\theta_i}} B^{1/2}XC^{-1/2}\tilde{\mathbf{s}}_i^{(d)}. \tag{2.12}$$

Proof. First let us show that $\tilde{\mathbf{s}}_i^{(d)}$ are indeed the eigenvectors of $H_{(d)}$ with eigenvalues θ_i:

$$\begin{aligned} H_{(d)}\tilde{\mathbf{s}}_i^{(d)} &= C^{1/2}YXC^{-1/2}\frac{1}{\sqrt{-\theta_i}}C^{1/2}YB^{-1/2}\tilde{\mathbf{s}}_i = \frac{1}{\sqrt{-\theta_i}}C^{1/2}YB^{-1/2}\left(B^{1/2}XYB^{-1/2}\right)\tilde{\mathbf{s}}_i \\ &= \frac{1}{\sqrt{-\theta_i}}C^{1/2}YB^{-1/2}H\tilde{\mathbf{s}}_i = \theta_i\tilde{\mathbf{s}}_i^{(d)}. \end{aligned}$$

To show that $\|\tilde{\mathbf{s}}_i^{(d)}\| = 1$, we note that

$$\left\langle \tilde{\mathbf{s}}_i^{(d)}, \tilde{\mathbf{s}}_i^{(d)}\right\rangle = \frac{1}{-\theta_i}\left\langle C^{1/2}YB^{-1/2}\tilde{\mathbf{s}}_i, C^{1/2}YB^{-1/2}\tilde{\mathbf{s}}_i\right\rangle = 1,$$

by way of derivation (2.10).

Equation (2.12) follows from (2.11) and the fact that $(\theta_i, \tilde{\mathbf{s}}_i)$ is the eigenpair of $H = B^{1/2}XYB^{-1/2}$. ∎

The solutions to (2.7), (2.9) can be written according to eigendecomposition as

$$\tilde{\mathbf{u}} = \hat{h}_1^{-1/2}(\lambda\mathbb{I} - H)^{-1}\mathbf{e}_1 = \hat{h}_1^{-1/2}\sum_{i=1}^{k}\frac{\tilde{s}_{i,1}}{\lambda - \theta_i}\tilde{\mathbf{s}}_i, \tag{2.13}$$

$$\tilde{\mathbf{v}} = -\frac{1}{\sqrt{\lambda}}\hat{h}_1^{-1}h_1^{-1/2}\left(\lambda\mathbb{I} - H_{(d)}\right)^{-1}\mathbf{e}_1 = -\frac{1}{\sqrt{\lambda}}\hat{h}_1^{-1}h_1^{-1/2}\sum_{i=1}^{k}\frac{\tilde{s}_{i,1}^{(d)}}{\lambda - \theta_i}\tilde{\mathbf{s}}_i^{(d)}, \tag{2.14}$$

where $\tilde{s}_{i,1}$ and $\tilde{s}_{i,1}^{(d)}$ are the first components of $\tilde{\mathbf{s}}_i$ and $\tilde{\mathbf{s}}_i^{(d)}$, respectively.

It is convenient to define the vectors $\mathbf{s}_i = B^{-1/2}\tilde{\mathbf{s}}_i$ and $\mathbf{s}_i^{(d)} = C^{-1/2}\tilde{\mathbf{s}}_i^{(d)}$, and note that

$$\begin{aligned} XY\mathbf{s}_i &= \theta_i\mathbf{s}_i, \quad YX\mathbf{s}_i^{(d)} = \theta_i\mathbf{s}_i^{(d)}, \\ \langle \mathbf{s}_i, B\mathbf{s}_j\rangle &= \delta_{ij}, \quad \left\langle \mathbf{s}_i^{(d)}, C\mathbf{s}_j^{(d)}\right\rangle = \delta_{ij}, \\ \sqrt{-\theta_i}\mathbf{s}_i^{(d)} &= Y\mathbf{s}_i, \quad \sqrt{-\theta_i}\mathbf{s}_i = -X\mathbf{s}_i^{(d)}, \end{aligned} \tag{2.15}$$

where formulas (2.11), (2.12) and (2.13), (2.14) are used, and δ_{ij} is Kronecker's symbol. With these definitions, the solutions to systems (2.6) and (2.8) are now written as

$$\mathbf{u} = B^{-1/2}\tilde{\mathbf{u}} = \sum_{i=1}^{k} \frac{s_{i,1}}{\lambda - \theta_i}\mathbf{s}_i, \tag{2.16}$$

$$\mathbf{v} = C^{-1/2}\tilde{\mathbf{v}} = -\frac{1}{\sqrt{\lambda}}\hat{h}_1^{-1}\sum_{i=1}^{k} \frac{s_{i,1}^{(d)}}{\lambda - \theta_i}\mathbf{s}_i^{(d)}. \tag{2.17}$$

Finally, we briefly describe the problem with the Neumann boundary condition on the "far" end. For it, the boundary conditions to system (2.3) are $u_{k+1} = u_k$, or, equivalently, $v_k = 0$, and hence (formally keeping v_k as an unknown variable) we make the following formal change in (2.3): the step h_k is set to be infinite. The rest of the above analysis remains unchanged.

2.2. The Equidistant Scheme

The finite difference scheme (2.3) with potential and derivative nodes spaced on the same distance from each other, i.e., a scheme with

$$\hat{h}_1 = h_k = h/2, \quad h_i = \hat{h}_j = h, \quad i = 1, \ldots, k-1, \quad j = 2, \ldots, k,$$

is called equidistant. (For the Neumann problem the step h_k above is infinite.)

Of course, the analysis above is fully applicable to the equidistant scheme, as well as one with varying grid steps. However, to distinguish the equidistant scheme from the rest, we change the notation slightly. Throughout this paper, the quantities referring to the equidistant scheme will carry subscripts (eq), and, moreover, the matrix $H_{(\mathrm{eq})}$ will be named A and its eigenvectors will be called $\tilde{\mathbf{z}}_i$ and eigenvalues a_i.

The analytic expression for the eigenvalues of A is

$$a_i = -\frac{4}{h^2}\sin^2\left(\frac{hl\pi}{4}\right), \quad i = 1, \ldots, N,$$

with the parameters $l = 2(i-1)$ and $l = 2(i-1)+1$ corresponding to the Neumann and Dirichlet schemes, respectively. The eigenvectors' components are given by

$$\tilde{z}_{i.j} = \chi_i \cos[(j-1)hl\pi/2], \quad i = 1, \ldots, N, \quad j = 1, \ldots, N,$$

with the same values of l, and $\chi_i = \sqrt{2}$ for $i = 2, \ldots, N-1$, for both Neumann and Dirichlet, and $\chi_1 = \sqrt{2}$, $\chi_N = 1$ for Neumann, $\chi_1 = 1$, $\chi_N = \sqrt{2}$ for Dirichlet.

2.3. Finite-Difference and Spectral Galerkin Approximations

Generally, the scheme (2.3) has second-order global convergence. However, it was shown in [8] that there exists a set of grid steps h_i and h_i independent of λ such that the finite-difference solution at the boundary becomes algebraically equivalent to the one of the polynomial spectral Galerkin method for all λ, and so it converges exponentially. Moreover, it is possible to construct a transformation of type (1.1) that transforms the finite-difference

solution to the polynomial spectral Galerkin one globally. In [8] this approach was proposed but not implemented numerically. Here we briefly outline this concept.

Let us solve the continuous problem using the standard spectral Galerkin method on the k-dimensional polynomial subspace span $\{x - L, (x - L)^3, \ldots, (x - L)^{2k+1}\}$. If we denote by η_i and z_i respectively the eigenvalues and eigenfunctions of the spectral Galerkin approximation (the Ritz eigenpairs), then the solution of the latter can be represented as

$$u_G(x) = \sum_{i=1}^{k} \frac{z_i(0) z_i(x)}{\lambda - \eta_i}. \tag{2.18}$$

Obviously, u_G converges to u exponentially for all $x \in [0, L]$. At the boundary $x = 0$ the spectral Galerkin solution can be represented as

$$u_G(0) = f_G(\lambda) = \sum_{i=1}^{k} \frac{z_i(0)^2}{\lambda - \eta_i},$$

where f_G is a so-called Galerkin–Petrov impedance function (the Neumann-to-Dirichlet map). It can be shown that f_G is the simple Padé approximant at $\lambda = 0$ to the true impedance function of (2.2), $u(0) = f(\lambda)$.

Using (2.16), we can define the discrete impedance function of (2.3) as

$$u_{k,1} = f_k(\lambda) = \sum_{i=1}^{k} \frac{s_{i,1}^2}{\lambda - \theta_i}.$$

The next step is to find h_i and $\hat{h}_i$ such that $\theta_i = \eta_i$ and $s_{i,1}^2 = z_i(0)^2$. So we construct a finite-difference scheme with $f_k \equiv f_G$. This is the same as solving an inverse impedance problem for a string of k unknown point masses $\hat{h}_i$ and weightless springs with stifnesses h_i (see Appendix B for details).

From the spectral representations (2.18), (2.16) follows the global expansion formula

$$u_G(x) = \sum_{i=1}^{k} z_i(x) \langle \mathbf{u}_k, B\mathbf{s}_i \rangle.$$

This formula transforms the finite-difference solution $\mathbf{u}_k$ to the spectral Galerkin solution $u_G(x)$. The inverse transform (reduction) can be written as

$$\mathbf{u}_k = \sum_{i=1}^{k} \left[\int_0^L u_G(x) z_i(x)\, dx \right] \mathbf{s}_i.$$

Since the above transforms do not explicitly depend on λ, they can be used in the time domain and in multidimensional problems.

The above approach would allow us to obtain spectral convergence using only the simple two-point approximation of the first derivatives. However, instead of the polynomial spectral Galerkin impedance functions f_G we will use the Padé–Chebyshev approximant to the true impedance. The reason for this is that the Padé–Chebyshev approximant is near optimal on large spectral intervals [3] and allows one to approach the theoretical limit of two points per wavelength, known as the Nyquist limit [2, 7]. We note the well-known fact that the corresponding limit of the polynomial spectral Galerkin method is π points per wavelength.

3. CONSTRUCTION OF THE OPTIMAL GRID

Our goal here is to construct a sequence $(h_i, \hat{h}_i)$ of steps for system (2.3) so that the impedance $u_{k,1}$ of the solution $\mathbf{u}_k$ approximates the impedance $u_{N,1}$ of the solution $\mathbf{u}_N$ of the equidistant scheme with a given step h. In fact, we define the equidistant grid by providing two parameters: the number N_w of minimum wavelengths in the physical region $[0, L]$ in question and the number P_w of points per minimum wavelength. It is essential that the Neumann and the Dirichlet equidistant problems are solved on the same grid; we choose the grid with the step $h = (2L)/(2N - 1)$, with $N = N_w P_w$. We are seeking the approximation of the impedances on a given spectral interval $\lambda \in [\lambda_1, \lambda_2]$ with $\lambda_2 = 0$, and we call n the number of eigenvalues a_i of A that fall onto that interval.

Recalling (2.16) and the notation chosen for the equidistant scheme, we obtain an expression for the impedance of the equidistant grid,

$$u_{N,1} = f_N(\lambda) = \sum_{i=1}^{N} \frac{z_{i,1}^2}{\lambda - a_i} = \hat{f}_N(\lambda) + \bar{f}_N(\lambda),$$

where $\bar{f}_N$ denotes the smooth part of f_N on the spectral interval, i.e., the part of the sum running from $n + 1$ to N.

For the optimal scheme being sought, we have

$$u_{k,1} = f_k(\lambda) = \sum_{i=1}^{N} \frac{s_{i,1}^2}{\lambda - \theta_i}.$$

We construct an approximation $f_k(\lambda)$ to $f_N(\lambda)$ of the form $f_k(\lambda) = \hat{f}_N(\lambda) + \bar{f}_k(\lambda)$, where

$$\bar{f}_k(\lambda) = \sum_{j=1}^{k-n} \frac{y_j}{\lambda - \eta_j}, \tag{3.1}$$

is a good approximation to the smooth part of the "equidistant" impedance $\bar{f}_N(\lambda)$. (In other words, we match the poles of the function under approximation on the given spectral interval exactly and approximate only the smooth part on that interval).

Having obtained all the k eigenvalues of H and the first components of all its eigenvectors (respectively, θ_i and $s_{i,1}$), we can proceed to obtain the optimal grid steps by solving the inverse spectral problem (see Appendix B).

3.1. Padé–Chebyshev Approximation

The approximation of the smooth part can be performed by various methods; we choose the Padé–Chebyshev approximant, i.e., the function $\bar{f}_k$ with the first $2(k - n) - 1$ Chebyshev coefficients coinciding with those of $\bar{f}_N$. Since in the sections explaining the expansion/reduction procedures we will need the apparatus required in the procedure of finding $\bar{f}_k$ and the following reconstruction of the "optimal" steps we will next concentrate on these procedures.

We want to construct the $[(m-1)/m]$ rational approximant $\bar{f}_k(\lambda)$ to $\bar{f}(\lambda)$ on the interval $[\lambda_1, \lambda_2]$ with $\bar{f}_k$ as in (3.1) with $m = k - n$ and $\bar{f}(\lambda)$ having a general form

$$\bar{f}(\lambda) = \int_{-\infty}^{0} (\lambda - x)^{-1}\, d\tau(x), \tag{3.2}$$

and with $\tau(x)$ a positive discrete measure on $(-\infty, 0]$. The general theory of Stieltjes integral is considered in [15, Chap. 6]. In this paper we only deal with piecewise constant nondecreasing functions τ having a finite number of jump points b_j with (positive) jumps a_j, i.e., $\tau(x) = \sum_{j:\, b_j \le x} a_j$, with $a_j, b_j \in \mathbb{R}$, $a_j > 0$, and $d\tau(x) = \sum_j a_j \delta(x - b_j)$.

We must now find parameters y_j, η_j, such that the first $2m$ Chebyshev coefficients of the functions $\bar{f}$ and $\bar{f}_k$, adjusted to the spectral interval $[\lambda_1, \lambda_2]$, coincide, which is the definition of the Padé–Chebyshev approximant. Obviously, matching the truncated Chebyshev series instead of the Taylor one as in the simple Padé yields better convergence of the approximant on the interval. Similarly to the simple Padé, the Padé–Chebyshev approximant can be computed in terms of Gaussian quadratures and Stiletjes moments [3].

Below we outline the material presented in more detail in [6].

To find the Padé–Chebyshev approximant, we first transform the interval $[\lambda_1, \lambda_2]$ in question into $[-1, 1]$ by making the change of variables $\lambda = [\lambda_1(1-\mu) + \lambda_2(1+\mu)]/2$.

Introduce the Zhukovsky function $\psi(t) = (t + t^{-1})/2$, $t \neq 0$ and its inverse $\Phi(z) = z + \sqrt{z^2 - 1}$, $\Phi(z) > 0$ for $z \in \mathbb{R}, z > 1$. Using the Chebyshev series for a simple pole (see [14, Sect. 10, (38)] or [1, 22.9.9]), we get

$$(\lambda - x)^{-1} = \frac{2}{\lambda_2 - \lambda_1} \left\{ -\frac{4\kappa(x)}{1 - \kappa(x)^2} {\sum_{l=0}^{\infty}}' \kappa(x)^l T_l[\mu(\lambda)] \right\}, \tag{3.3}$$

where T_i are Chebyshev's polynomials, the prime symbol means that the term for $l = 0$ is to be divided by 2, and

$$\kappa(x) = \Phi\left[\frac{2x - (\lambda_2 + \lambda_1)}{\lambda_2 - \lambda_1} \right]^{-1}. \tag{3.4}$$

By the use of the formulas (3.2) and (3.3) and some manipulations one can present the lth Chebyshev coefficient c_l of the function $\bar{f}$ with the shifted argument as

$$c_l[\bar{f}] = -\frac{8}{\lambda_2 - \lambda_1} \int_{-\infty}^{0} \frac{\kappa(x)}{1 - \kappa(x)^2} \kappa(x)^l\, d\tau(x).$$

Let

$$\rho = -\Phi\left(-\frac{\lambda_2 + \lambda_1}{\lambda_2 - \lambda_1} \right)^{-1}, \quad 0 < \rho < 1,$$

and make the change of variables $t = \kappa(x)$; then

$$c_l[\bar{f}] = \frac{8}{\lambda_2 - \lambda_1} \int_{-\rho}^{0} t^l\, d\tilde{\tau}(t),$$

with $\tilde{\tau}(t)$ a positive measure on $[-\rho, 0]$ such that

$$\tilde{\tau}(t) = \sum\nolimits_{j:\,\kappa(b_j)\le t} \frac{-a_j\kappa(b_j)}{1-\kappa(b_j)^2}.$$

The analogous expression for $\bar{f}_k(\lambda)$ is

$$c_l[\bar{f}_k] = -\frac{8}{\lambda_2-\lambda_1}\sum_{j=1}^{m}\frac{y_j\zeta_j}{1-\zeta_j^2}\zeta_j^l, \quad \text{with } \zeta_j = \kappa(\eta_j).$$

It follows that the formal condition on y_j, η_j for a rational function $\bar{f}_k(\lambda)$ to be the $[(m-1)/m]$ Padé–Chebyshev approximant to $\bar{f}(\lambda)$ is

$$\int_{-\rho}^{0} t^l\, d\tilde{\tau}(t) = -\sum_{j=1}^{m}\frac{y_j\zeta_j}{1-\zeta_j^2}\zeta_j^l, \quad l = 0, 1, \ldots, 2m-1. \tag{3.5}$$

This is a moment problem of the type (A.9), considered in Appendix A.

To find the function $\bar{f}_k$, we perform the Lanczos process (see Appendix A) in the linear space $\mathbb{R}[t]$, supplied with the inner product $\langle .,. \rangle$ determined by the measure $\tilde{\tau}$, i.e., $\langle p, q\rangle = \int_\rho^0 p(t)q(t)\, d\tilde{\tau}(t)$, $p, q \in \mathbb{R}[t]$, with the operator of multiplication by the independent variable t and the initial vector 1 (a constant polynomial). At the mth step we will have

$$\langle t^l, 1\rangle = \int_{-\rho}^{0} t^l\, d\tilde{\tau}(t) = \|1\|^2\langle T^l\mathbf{e}_1, \mathbf{e}_1\rangle = \|1\|^2\sum_{j=1}^{m} b_{j,1}^2 t_j^l, \tag{3.6}$$

for all $0 \le l \le 2m-1$. Here $(\mathbf{b}_j, t_j)$ are the eigenpairs of the Lanczos tridiagonal symmetric $m \times m$ matrix T and $\|1\|^2 = \langle 1, 1\rangle = \int_{-\rho}^{0} d\tilde{\tau}$.

Comparing (3.5) and (3.6), we see that the eigenpairs of T satisfy

$$t_j = \zeta_j, \quad b_{j,1}^2 = -\frac{y_j\zeta_j}{1-\zeta_j^2}\|1\|^{-2}. \tag{3.7}$$

We can thus easily determine η_j and y_j (the function (3.1) so defined is really Markov) and then use the expressions

$$s_{j+n,1}^2 = y_j, \quad \theta_{j+n} = \eta_j. \tag{3.8}$$

3.2. Approximating the Continuous Impedance

The reader might notice that in our previous paper [2] we proposed the computation of the "optimal" finite-difference grid based on the approximation of the continuous impedance, rather than the approximation of the impedance of an equidistant scheme, as described above. The steps resulting from these two different approaches will be slightly different and, of course, the impedance of the former scheme will be more accurate (when compared to the analytic solution) than the latter.

There are two reasons for our change of mind.

The first reason is that the procedure of direct approximation of the true continuous impedance function generates the minimum step that is a little smaller than the step of the equidistant grid which produces the same error in the approximation of the impedance. Thus, in practice, when the resulting finite-difference scheme is to be used for solutions of time-domain equations and is to be implemented using explicit time-stepping, we find that the Courant–Frederix–Levy (CFL) stability condition of the so obtained optimal scheme is more restrictive than that of the corresponding equidistant scheme (the time step used in the optimal scheme producing an error of about 2% is approximately 10% smaller than the time step of the equidistant scheme giving the same accuracy, as reported in [2]). This fact makes the use of such an optimal grid less advantageous, for, even though the benefit of using a smaller amount of grid nodes is still present, the necessity of a smaller discretization time step negatively impacts the overall advantage in speed.

The approximation of the "equidistant" impedance proposed here cures this defect, as the minimum step of the optimal scheme obtained this way is no smaller than the step h of the equidistant grid, and thus the stability condition of the new scheme will be no more restrictive than that of the corresponding equidistant scheme. Indeed, the process of construction of the optimal mesh based on the Lanczos algorithm described above produces the matrix H for which the spectrum is included in the same interval as the spectrum of the original matrix A. Thus, the stability condition of the FD scheme that uses the new optimal steps is more relaxed than that of the original scheme.

The second reason is that this new approach allows us to pass from the solution of the equidistant scheme to the solution of the optimal scheme (and back) with minimal errors, by the procedures of "expansion" and "reduction," the details of which, as well as their importance and applications, are described below.

Of course, when these reasons are not of importance, one can successfully use the steps obtained by a process of Padé–Chebyshev approximation of the continuous impedance

$$u(0) = f(\lambda) = \frac{1 - e^{-2L\sqrt{\lambda}}}{\sqrt{\lambda}\left(1 + e^{-2L\sqrt{\lambda}}\right)} = \frac{2}{L}\sum_{i=1}^{\infty}\frac{1}{\lambda - \xi_i}, \quad \xi_i = -\left[\frac{\pi(i - 1/2)}{L}\right]^2.$$

The process of getting these steps is exactly the same: the poles of f that fall on the spectral interval in question are matched exactly, and the remaining smooth part is approximated using the algorithm of Section 3.1.

4. EXPANSIONS AND REDUCTIONS

We now present an algorithm for calculating an accurate approximation to the solution $u(x, \lambda)$ for the points $x = (i - 1)h$, $i = 1, \ldots, N$, corresponding to the nodes of the equidistant grid, by using the finite-difference solution produced by the optimal scheme. It is assumed here that the optimal grid steps are obtained by the Padé–Chebyshev approximation of the equidistant scheme currently under consideration.

To fix notation, consider the two spaces $\mathbb{R}^N$ and $\mathbb{R}^k$. In the following discussion, we will denote elements from the two spaces and corresponding matrix spaces (e.g., basis vectors, identity matrices, etc.) by the same names, only distinguishing them by sub- or superscripts N and k (or tags "op" for "optimal" and "eq" for "equidistant") wherever necessary.

Let A and H be defined as before, with the eigenpairs $(a_i, \tilde{\mathbf{z}}_i)$ and $(\theta_i, \tilde{\mathbf{s}}_i)$, respectively, and recall the notation for $\mathbf{s}_i = B_{(\mathrm{op})}^{-1/2}\tilde{\mathbf{s}}_i$, $\mathbf{z}_i = B_{(\mathrm{eq})}^{-1/2}\tilde{\mathbf{z}}_i$ (note that $\langle \mathbf{s}_i, B_{(\mathrm{op})}\mathbf{s}_j\rangle = \delta_{ij}$, $\langle \mathbf{z}_i, B_{(\mathrm{eq})}\mathbf{z}_j\rangle = \delta_{ij}$).

By construction of H, $\theta_i = a_i$ for $i \le n$, $S_{i,1} = z_{i,1}$ for $i \le n$. Here n is such that $a_i \in [\lambda_1, \lambda_2]$ for $i \le n$.

Let $\tilde{Z}$ be the matrix consisting of the vectors $\tilde{\mathbf{z}}_i$ as columns. Consider a decomposition of vector space $\mathbb{R}^N$ into an orthogonal sum of subspaces $\mathbb{R}_1^N = \mathrm{span}\{\tilde{\mathbf{z}}_1, \ldots, \tilde{\mathbf{z}}_n\}$ and $\mathbb{R}_2^N = \mathbb{R}^N \ominus \mathbb{R}_1^N$. Let $P_1 = \mathrm{diag}\{1, \ldots, 1, 0, \ldots, 0\}$, where the number of 1's on the diagonal is n, and $P_2 = \mathbb{I} - P_1$. We will write $\mathbf{b}^{(1)} = (\tilde{Z}P_1\tilde{Z}^T)\mathbf{b}$ and $\mathbf{b}^{(2)} = (\tilde{Z}P_2\tilde{Z}^T)\mathbf{b}$ for the projections onto subspaces $\mathbb{R}_1^N$ and $\mathbb{R}_2^N$ of any vector $\mathrm{b} \in \mathbb{R}^N$; obviously, $\mathbf{b} = \mathbf{b}^{(1)} + \mathbf{b}^{(2)}$.

We will also consider another decomposition of every vector in $\mathbb{R}^N$: if $\mathbf{a} = B_{(\mathrm{eq})}^{-1/2}\mathbf{b}$, then we will write $\mathbf{a} = \hat{\mathbf{a}} + \bar{\mathbf{a}}$, where $\hat{\mathbf{a}} = B_{(\mathrm{eq})}^{-1/2}\mathbf{b}^{(1)}$ and $\bar{\mathbf{a}} = B_{(\mathrm{eq})}^{-1/2}\mathbf{b}^{(2)}$.

All $N \times N$ matrices can also be decomposed as $M = M^{(1)} + M^{(2)}$, where

$$M^{(1)} = (\tilde{Z}P_1\tilde{Z}^T)M(\tilde{Z}P_1\tilde{Z}^T) \quad \text{and} \quad M^{(2)} = (\tilde{Z}P_2\tilde{Z}^T)M(\tilde{Z}P_2\tilde{Z}^T).$$

The corresponding decompositions of $\mathbb{R}^k$ can be obtained analogously if one takes instead of $\tilde{Z}$ the matrix $\tilde{S}$ consisting of the eigenvectors $\tilde{\mathbf{s}}_i$ of H as columns and takes $B_{(\mathrm{op})}$ instead of $B_{(\mathrm{eq})}$.

4.1. Expansions

We want to construct an approximation $\mathbf{u}_I$ to $\mathbf{u}_N$ such that

(i) $\hat{\mathbf{u}}_I = \hat{\mathbf{u}}_N$;
(ii) $\bar{\mathbf{u}}_I$ is a $(k-n)$-step Lanczos approximation to $\bar{\mathbf{u}}_N$;
(iii) the impedance of $\mathbf{u}_I$ is the same as that of $\mathbf{u}_k$, i.e., $\mathbf{u}_{I,1} = u_{k,1} = \sum_{i=1}^k s_{i,1}^2/(\lambda - \theta_i)$.

Condition (i) is easily satisfied by putting

$$\hat{\mathbf{u}}_I = \hat{\mathbf{u}}_N = B_{(\mathrm{eq})}^{-1/2}\tilde{\mathbf{u}}_N^{(1)} = \hat{h}_{1,(\mathrm{eq})}^{-1/2}B_{(\mathrm{eq})}^{-1/2}\sum_{i=1}^n \frac{\tilde{z}_{i,1}}{\lambda - a_i}\tilde{\mathbf{z}}_i = \sum_{i=1}^n \frac{z_{i,1}}{\lambda - a_i}\mathbf{z}_i = \sum_{i=1}^n \frac{s_{i,1}}{\lambda - \theta_i}\mathbf{z}_i. \quad (4.1)$$

To satisfy condition (ii), we first note that $\bar{\mathbf{u}}_N = B_{(\mathrm{eq})}^{-1/2}\tilde{\mathbf{u}}_N^{(2)}$ where $\tilde{\mathbf{u}}_N^{(2)} = \hat{h}_{1,(\mathrm{eq})}^{-1/2}(\lambda\mathbb{I} - A^{(2)})^{-1}\mathbf{e}_1$. So, a condition equivalent to (ii) would be that $\bar{\mathbf{u}}_I = B_{(\mathrm{eq})}^{-1/2}\tilde{\mathbf{u}}_I^{(2)}$ where $\tilde{\mathbf{u}}_I^{(2)}$ is a Lanczos approximation to $\tilde{\mathbf{u}}_N^{(2)}$. This approximation should be carefully devised so that the most important condition (iii) is satisfied.

CLAIM 4.1. *Let $g(x) = -x/(1-x^2)$, $d(x) = 1/g(x)$, $G = \kappa(A^{(2)})$, $\varphi = \hat{h}_{1,(eq)}^{-1/2}g(G)\mathbf{e}_1$, and $F(x) = [\lambda - \kappa(x)^{-1}]^{-1}d(x)$, where κ is defined by* (3.4). *Perform a Lanczos process to evaluate the approximation $\tilde{\mathbf{u}}_I^{(2)}$ to $\tilde{\mathbf{u}}_N^{(2)} = F(G)\varphi$ in $\mathbb{R}_2^N$ with the scalar product $\langle \mathbf{a}, \mathbf{b}\rangle_d = \langle \mathbf{a}, d(G)\mathbf{b}\rangle$; i.e., obtain the tridiagonal matrix $\hat{T}$ and the Lanczos matrix $Q = (\mathbf{q}_1, \ldots, \mathbf{q}_k)$. Then the matrix $\hat{T}$ coincides with the matrix T, obtained in the Lanczos process described in Section* 3, *and condition* (iii) *above is satisfied.*

To check that the two matrices are the same, we calculate the corresponding moments. The moments of the Lanczos process described in Section 3 are

$$\int_{-\rho}^0 t^l\, d\tilde{\tau}(t) = \int_{-\infty}^0 \kappa(x)^l \frac{-\kappa(x)}{1-\kappa(x)^2}\, d\tau(x) = \sum_{i=n+1}^N \frac{-\kappa(a_i)}{1-\kappa(a_i)^2}\kappa(a_i)^l z_{i,1}^2.$$

For the Lanczos process we are carrying now, eigendecomposition yields

$$\langle G^l\varphi,\varphi\rangle_d = \hat{h}^{-1}_{1,(\mathrm{eq})}\langle G^l g(G)\mathbf{e}_1, d(G)g(G)\mathbf{e}_1\rangle = \sum_{i=n+1}^{N} \kappa(a_i)^l g(\kappa(a_i))^2 d(\kappa(a_i)) z_{i,1}^2$$
$$= \sum_{i=n+1}^{N} \frac{-\kappa(a_i)}{1-\kappa(a_i)^2}\kappa(a_i)^l z_{i,1}^2.$$

Hence, the two tridiagonal matrices are equal.

The approximation $\tilde{\mathbf{u}}_I^{(2)}$ to $\tilde{\mathbf{u}}_N^{(2)}$ now takes the SLDM form (see Appendix A, formula (A.3))

$$\tilde{\mathbf{u}}_I^{(2)} = \|\varphi\|_d Q F(T)\mathbf{e}_1 = \|\varphi\|_d \sum_{j-1}^{k-n} b_{j,1} F(t_j)\xi_j, \tag{4.2}$$

where $\|\varphi\|_d = \sqrt{\langle\varphi,\varphi\rangle_d}$ and $\xi_j = Q\mathbf{b}_j$. For the norm of φ we have

$$\|\varphi\|_d^2 = \hat{h}^{-1}_{1,(\mathrm{eq})}\langle g(G)\mathbf{e}_1, d(G)g(G)\mathbf{e}_1\rangle = \hat{h}^{-1}_{1,(\mathrm{eq})}\langle g(G)\mathbf{e}_1,\mathbf{e}_1\rangle$$
$$= \hat{h}^{-1}_{1,(\mathrm{eq})}\sum_{i=n+1}^{N} g(\kappa(a_i))\tilde{z}_{i,1}^2 = \sum_{i=n+1}^{N}\frac{-\kappa(a_i)}{1-\kappa(a_i)^2}z_{i,1}^2$$
$$= \int_{-\infty}^{0}\frac{-\kappa(x)}{1-\kappa(x)^2}\,d\tau = \int_{-\rho}^{0} d\tilde{\tau} = \|1\|^2,$$

where 1 is the initial vector for the Lanczos process considered in Section 3.1. We thus obtain

$$g(t_j) = \frac{-t_j}{1-t_j^2} = \left(\frac{-y_j t_j}{1-t_j^2}\right)\frac{\|\varphi\|_d^2}{\|1\|^2}\left(\frac{1}{y_j}\right) = \frac{b_{j,1}^2}{s_{j+n,1}^2}\|\varphi\|_d^2,$$

where (3.7) and (3.8) were used, and hence

$$F(t_j) = \frac{1}{\lambda-\kappa(t_j)^{-1}}g(t_j)^{-1} = \frac{s_{j+n,1}^2}{(\lambda-\theta_{j+n})b_{j,1}^2\|\varphi\|_d^2}.$$

Calculating the first component of the vector $\tilde{u}_I^{(2)}$, we get

$$\begin{aligned}
\tilde{u}_{I,1}^{(2)} &= \|\varphi\|_d\sum_{j=1}^{k-n} F(t_j)b_{j,1}\langle\xi_j,\mathbf{e}_1\rangle \\
&= \|\varphi\|_d\hat{h}^{1/2}_{1,(\mathrm{eq})}\sum_{j=1}^{k-n} F(t_j)b_{j,1}\langle\mathbf{b}_j,\, Q^T d(G)\varphi\rangle \\
&= \|\varphi\|_d^2\hat{h}^{1/2}_{1,(\mathrm{eq})}\sum_{j=1}^{k-n} F(t_j)b_{j,1}^2 \\
&= \hat{h}^{1/2}_{1(\mathrm{eq})}\sum_{j=1}^{k-n}\frac{s_{j+n,1}^2}{\lambda-\theta_{j+n}}.
\end{aligned} \tag{4.3}$$

Now, since $\bar{u}_{I,1} = \langle B_{(\mathrm{eq})}^{-1/2}\tilde{\mathbf{u}}_I^{(2)}, \mathbf{e}_1\rangle = \hat{h}_{1,(\mathrm{eq})}^{-1/2}\tilde{u}_{I,1}^{(2)}$, the impedance of the "bar" part of the approximate solution is given by

$$\bar{u}_{I,1} = \sum_{j=1}^{k-n} \frac{s_{j+n,1}^2}{\lambda - \theta_{j+n}},$$

which, together with (4.1), implies condition (iii).

Overall, the expression for $\bar{\mathbf{u}}_I$ is

$$\begin{aligned}\bar{\mathbf{u}}_I &= B_{(\mathrm{eq})}^{-1/2}\|\varphi\|_d \sum_{j=1}^{k-n} \xi_j F(t_j) b_{i,1} = B_{(\mathrm{eq})}^{-1/2} \sum_{j=1}^{k-n} \xi_j \frac{s_{j+n,1}^2}{b_{j,1}\|\varphi\|_d(\lambda - \theta_{j+n})} \\ &= \sum_{j=1}^{k-n} \frac{s_{j+n,1}}{\lambda - \theta_{j+n}} B_{(\mathrm{eq})}^{-1/2}\xi_j \left(\frac{s_{j+n,1}}{b_{j,1}}\frac{1}{\|\varphi\|_d}\right) = \sum_{j=1}^{k-n} B_{(\mathrm{eq})}^{-1/2}\xi_j \frac{s_{j+n,1}}{\lambda - \theta_{j+n}} g(t_j)^{-1/2}.\end{aligned}$$

Thus the final form of approximation $\mathbf{u}_I$ is

$$\mathbf{u}_I = \sum_{i=1}^{n} \frac{s_{i,1}}{\lambda - \theta_i}\mathbf{z}_i + \sum_{j=1}^{k-n} \alpha_j \frac{s_{j+n,1}}{\lambda - \theta_{j+n}}\beta_j, \tag{4.4}$$

with

$$\alpha_j = g(t_j)^{-1/2}, \quad \beta_j = B_{(\mathrm{eq})}^{-1/2}\xi_j.$$

Using the fact that $\langle \mathbf{u}_k, B_{(\mathrm{op})}\mathbf{s}_i\rangle = s_{i,1}/(\lambda - \theta_i)$, we can rewrite (4.4) as

$$\mathbf{u}_I = \sum_{i=1}^{n} \big\langle \mathbf{u}_k, B_{(\mathrm{op})}\mathbf{s}_i\big\rangle \mathbf{z}_i + \sum_{j=1}^{k-n} \alpha_j \big\langle \mathbf{u}_k, B_{(\mathrm{op})}\mathbf{s}_{j+n}\big\rangle \beta_j. \tag{4.5}$$

One can now see that the approximation does not depend on λ explicitly, and hence it can be easily transformed into the time domain. The vector $\mathbf{u}_I$ is called the *expansion* of the optimal solution $\mathbf{u}_k$ into the space $\mathbb{R}^N$. So, (4.5) is equivalent to (1.1).

4.2. Reductions

We now present a procedure that in some sense is an inverse to the expansion, i.e., starting from the solution of the equidistant scheme (residing in space $\mathbb{R}^N$), we construct an approximation to the solution of the corresponding optimal scheme (in space $\mathbb{R}^k$). Analogously to the term "grid reduction" we call this procedure a *reduction*.

We first note that, by construction,

$$\big\langle \mathbf{z}_i, B_{(\mathrm{eq})}\mathbf{z}_j\big\rangle = \delta_{ij}, \quad \big\langle \mathbf{z}_i, B_{(\mathrm{eq})}\beta_l\big\rangle = 0, \quad \text{for } i, j \le n, \quad l \le k - n,$$

and

$$\langle \beta_i, W\beta_j\rangle = \delta_{ij}, \quad \big\langle \beta_i, W_{\mathbf{z}_l}\big\rangle = 0, \quad \text{for } l \le n, \quad i, j \le k - n,$$

where $W = B_{(\mathrm{eq})}^{1/2} Q Q^T B_{(\mathrm{eq})}^{1/2}$ (recall that, in general, $QQ^T \ne \mathbb{I}$.)

We thus have, according to (4.5),

$$\left\langle \mathbf{u}_I,\, B_{(\mathrm{eq})}\mathbf{z}_i \right\rangle = \left\langle \mathbf{u}_k,\, B_{(\mathrm{op})}\mathbf{s}_i \right\rangle, \quad i = 1, \ldots, n,$$

and

$$\langle \mathbf{u}_I,\, W\beta_j \rangle = \alpha_j \left\langle \mathbf{u}_k,\, B_{(\mathrm{op})}\mathbf{s}_{j+n} \right\rangle, \quad j = 1, \ldots, n-k.$$

Hence the formula for getting the "optimal" solution back from the expanded one is

$$\mathbf{u}_k = \sum_{i=1}^{n} \left\langle \mathbf{u}_I,\, B_{(\mathrm{eq})}\mathbf{z}_i \right\rangle \mathbf{s}_i + \sum_{j=1}^{n-k} \alpha_j^{-1} \langle \mathbf{u}_I,\, W\beta_j \rangle \mathbf{s}_{j+n}. \tag{4.6}$$

This formula is exact, but if we change the expanded solution $\mathbf{u}_I$ above to the true solution $\mathbf{u}_N$ of the equidistant scheme, we will get on the left of the above equation the "reduced" solution, which is equal to $\mathbf{u}_k$ only approximately.

Formulas (4.5) and (4.6) allow us to pass from the finite-difference solution defined on the optimal grid to the one defined on the equidistant grid with minimal errors.

4.3. Expansion/Reduction for the Dual Problem

What happens if one wants to expand the derivatives of the finite-difference solution, i.e., the data that are placed at the "derivative" nodes $\hat{x}_i$? This question is very important, for when the simple scalar problem currently under consideration is changed to a vector problem, e.g., the equations of elasticity, data at "potential" nodes and data at "derivative" nodes are no longer connected by a simple finite differentiation, and an updated expansion procedure is necessary.

Having constructed the approximation $\mathbf{u}_I \approx \mathbf{u}_N$, given by (4.5), we want to compute the expansion of the solution $\mathbf{v}_N = \frac{1}{\sqrt{\lambda}} Y_{(\mathrm{eq})}\mathbf{u}_N$. We wish the approximant $\mathbf{v}_I$ to be calculated directly from the solution $\mathbf{v}_k$ of the optimal scheme, rather than from the expanded potential solution u_I.

Considering (4.5), we easily construct

$$\mathbf{v}_I = \frac{1}{\sqrt{\lambda}} \sum_{i=1}^{n} \left(Y_{(\mathrm{eq})}\mathbf{z}_i\right) \left\langle \mathbf{u}_k,\, B_{(\mathrm{op})}\mathbf{s}_i \right\rangle + \frac{1}{\sqrt{\lambda}} \sum_{j=1}^{k-n} \alpha_j \left(Y_{(\mathrm{eq})}\beta_j\right) \left\langle \mathbf{u}_k,\, B_{(\mathrm{op})}\mathbf{s}_{j+n} \right\rangle.$$

Recalling that $\frac{1}{\sqrt{\lambda}}\mathbf{u}_k = Y_{(\mathrm{op})}^{-1}\mathbf{v}_k$, we get

$$\left\langle \frac{1}{\sqrt{\lambda}}\mathbf{u}_k,\, B_{(\mathrm{op})}\mathbf{s}_i \right\rangle = \left\langle \mathbf{v}_k,\, Y_{(\mathrm{op})}^{-T} B_{(\mathrm{op})}\mathbf{s}_i \right\rangle = \left\langle \mathbf{v}_k,\, C_{(\mathrm{op})} \left[C_{(\mathrm{op})}^{-1} Y_{(\mathrm{op})}^{-T} B_{(\mathrm{op})}\right]\mathbf{s}_i \right\rangle.$$

But it follows from (2.5) and (2.15) that

$$C_{(\mathrm{op})}^{-1} Y_{(\mathrm{op})}^{-T} B_{(\mathrm{op})}\mathbf{s}_i = -X_{(\mathrm{op})}^{-1}\mathbf{s}_i = \frac{1}{\sqrt{-\theta_i}}\mathbf{s}_i^{(d)};$$

hence, we get the final formula for the expansion of the dual problem,

$$\mathbf{v}_I = \sum_{i=1}^{n} \left\langle \mathbf{v}_k,\, C_{(\mathrm{op})}\mathbf{s}_i^{(d)} \right\rangle \mathbf{z}_i^{(d)} + \sum_{j=1}^{k-n} \frac{\alpha_j}{\sqrt{-\theta_{j+n}}} \left\langle \mathbf{v}_k,\, C_{(\mathrm{op})}\mathbf{s}_{j+n}^{(d)} \right\rangle Y_{(\mathrm{eq})}\beta_j,$$

and the inverse formula (dual reduction) takes the form

$$\mathbf{v}_k = \sum_{i=1}^{n} \left\langle \mathbf{v}_I, C_{(\mathrm{eq})}\mathbf{z}_i^{(d)} \right\rangle \mathbf{s}_i^{(d)} + \sum_{j=1}^{k-n} \frac{\sqrt{-\theta_{j+n}}}{\alpha_j} \left\langle \mathbf{v}_I, WY_{(\mathrm{eq})}\beta_j \right\rangle \mathbf{s}_{j+n}^{(d)}.$$

4.4. Error Considerations

Formula (4.2) shows that $\tilde{\mathbf{u}}_I^{(2)}$ is the SLDM solution for the Lanczos process applied to F and φ, at step $k-n$, whereas (4.3) demonstrates that $\tilde{u}_{I,1}^{(2)}$ is the Gaussian quadrature approximation for the same Lanczos process. In [12, Section 5.1] the error estimates, formulated in terms of Chebyshev coefficients of a function F, for SLDM (see Theorem 1) and Gaussian quadrature associated with a Lanczos process (see Theorem 2) were compared. It was proved that the former error bound at the mth step is close to the latter error bound at the $2m$th step. Hence, $\tilde{u}_{I,1}^{(2)}$ is expected to converge twice as fast as $\tilde{\mathbf{u}}_I^{(2)}$. Notwithstanding that the actual errors may be essentially less than the corresponding upper bounds, our experience has shown that the conclusion derived from the considered estimates is qualitatively realistic.

4.5. Experiment 1

To demonstrate the effectiveness of the transformation processes described above, we consider the following example: we solve a one-dimensional scalar wave problem in the time domain on $x \in [0, 1]$, with a source positioned at $x = 0.5$. In two separate experiments we employ two different meshes: the equidistant one with 32 points per minimum wavelength (or 576 nodes in total on $[0, 1]$) and the optimal one, which is constructed to match the same impedance (it turns out that the optimal mesh has a total of 58 nodes). Specifically, in the experiment in which the optimal mesh was employed, the optimal mesh was calculated as explained above for the range $[0, 1]$ and then scaled from that range to $[0, 0.5]$ and taken to be symmetric around $x = 0.5$.

In Fig. 3 one can see the signal recorded at $x = 0.5$ for both experiments—the waves are indistinguishable (in fact, the $L^2(t)$ error between the two signals is less than 0.5%, which cannot be seen on the graph). It is noticeable that the recorded signal is not very accurate by itself: there is obvious dispersion present, and the signal peaks do not all have the same magnitude; nevertheless, the difference between the solution computed on the optimal mesh and that on the equidistant mesh is small.

At this stage no expansion or reduction was used (or needed), because the signals were recorded at the same point where the source was introduced, i.e., at the point which was specially chosen to be producing the good accuracy.

Figure 4 shows the behavior of the solution at a certain time for all x. The grid nodes of the optimal mesh are shown by the black dots; the nodes of the equidistant mesh are not shown as they would be indistinguishably close to each other. One can see that the behavior of the optimal solution at points remote from the "receiver" is incredibly irregular and inaccurate, compared to the one computed on the equidistant grid.

However, in fact there are not two, but four graphs present in Fig. 4: the solution on each mesh, the expansion of the optimal solution, and the reduction of the equidistant one. These transformed solutions are so close to their true counterparts on the corresponding mesh that one cannot differentiate them on the picture ($L^2(x)$ error is again less than 0.5%).

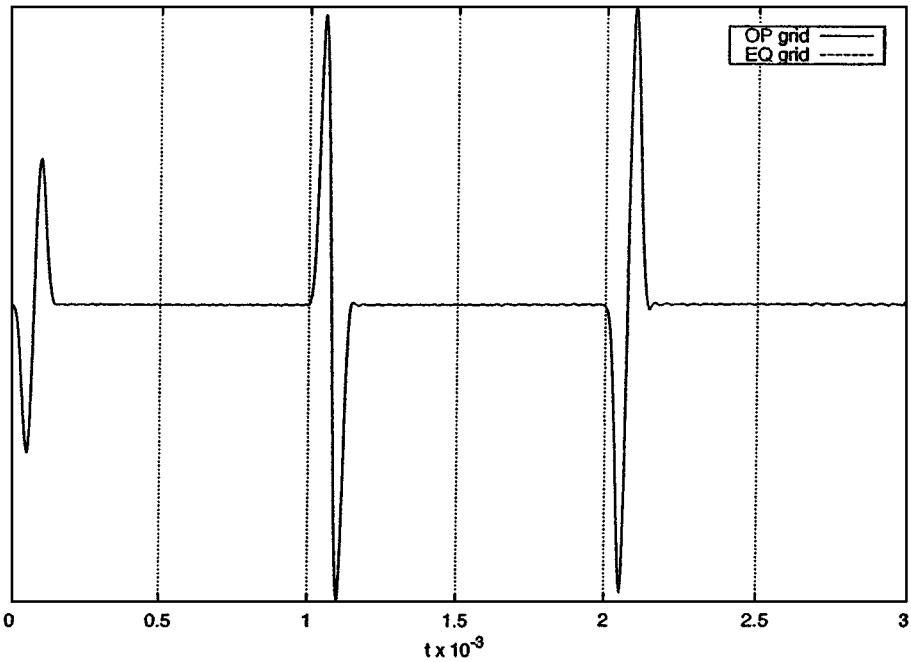

FIG. 3. Recorded signal for Experiment 1.

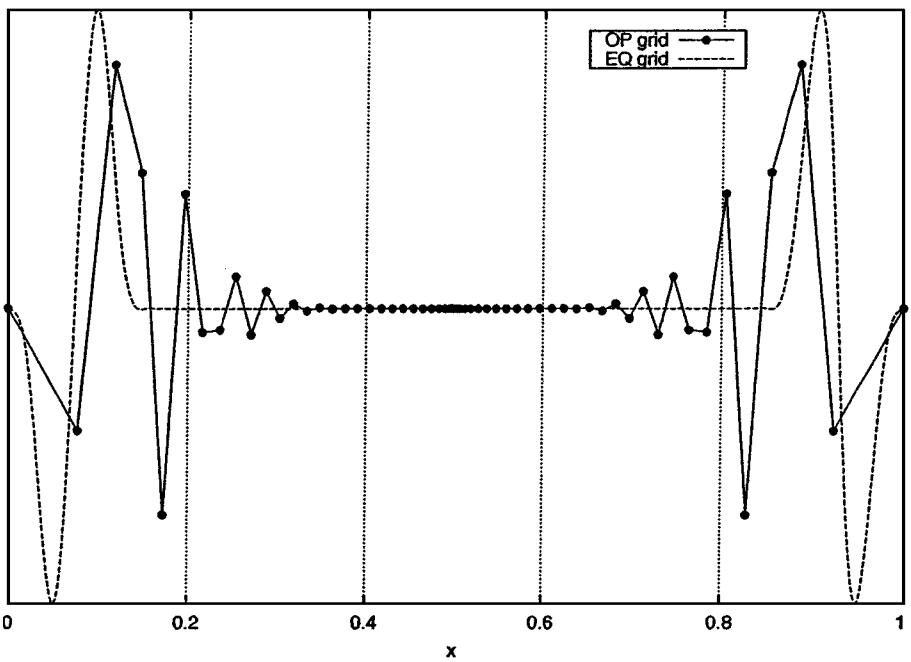

FIG. 4. Behavior of the optimal and equidistant solutions for Experiment 1 as functions of x for a certain time.

This experiment demonstrates that when one needs to compute the solution of a hyperbolic equation at all times at a certain point, the use of the optimal mesh can decrease the amount of computation by as much as an order of magnitude over the use of the equidistant mesh, with no loss in accuracy. Moreover, when there is a need to compute the solution on the whole 1D computational domain (or a 1D subdomain of a larger-dimensional domain) at a certain time, the process of expansion is the tool that does the job.

5. NONMATCHING GRIDS: EXTENSION TO 2.5D CYLINDRICAL ELASTICITY

As another practical application of the transformation procedures described in the previous section we propose the following idea. Suppose the computational domain (which we can deem 2D or 3D by means of taking tensor product grids; see [2]) consists of several regions, some of which have densely varying media, while the others have media parameters varying on a larger scale. It would seem natural to grid the densely changing "blocks" (or subdomains) with a standard equidistant grid and perform standard averaging of media parameters there, while leaving the constant "blocks" gridded with a much coarser optimal mesh (on which, unfortunately, the averaging of media parameters does not currently work and is a field of current research). The conjugation conditions that are employed on the interfaces between optimal and equidistant regions require the use of expansion and reduction procedures while passing between the solution on one side to the solution at the other side for both the potential and derivative nodes on the grid.

Although on each of the described subregions the grid remains a tensor product, the resulting *global* grid will *not* be a tensor product. We call such grids nonmatching.

The proposed scheme can be easily extended for computing solutions of equations of linear elastodynamics. We developed a program that solves these equations written in cylindrical coordinates, for the so-called 2.5D case [2]. This program is used for geophysical tasks such as computing acoustic responses of various tools in cylindrical borehole environment. The program allows for arbitrary rectangular decomposition of the (r, z)-computational domain, with an arbitrary optimal or equidistant choice for the gridding of each of the resulting subdomains in the z direction (the grid in the non-Cartesian r direction is kept equidistant throughout). The resulting globally non-tensor-product grid is essential when the tool under consideration is finely detailed, while the parameters of the surrounding formations are varying on a larger scale. A sketch of such a configuration is presented in Fig. 5. Here, the "borehole" region (on the left in the picture) is gridded in the equidistant fashion (the grid is shown in the vertical direction only), while the rest of the computational domain is gridded with an optimal mesh, with the processes of expansion and reduction performed on the vertical interface between the regions for conjugation at every time step.

5.1. Experiment 2

To demonstrate the effectiveness of the proposed techniques, we compare the times spent on computing acoustic responses of the tool with the geometry presented in Fig. 6 (the figure is not drawn to scale; the r/z scale ratio is $1:20$). We compare the times used to compute the solution on the nonmatching grid to the ones that were required to compute the same

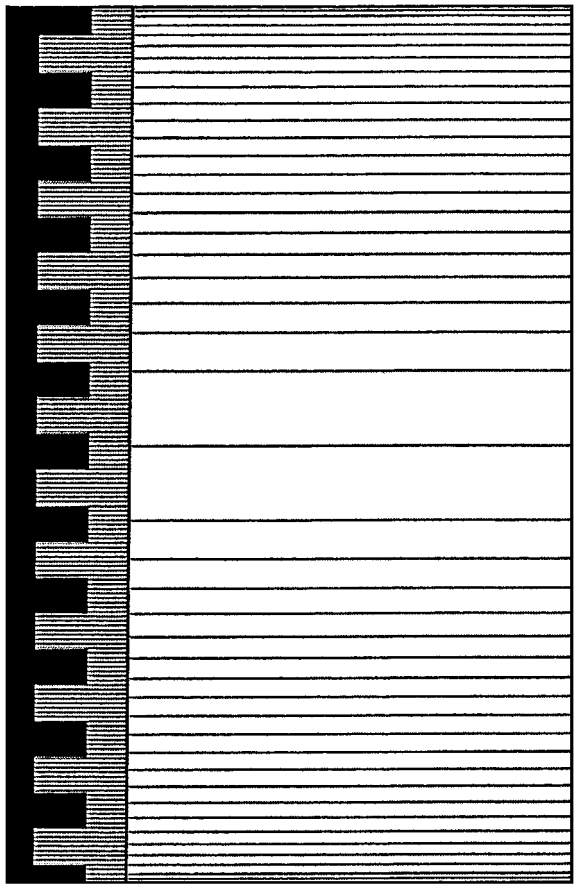

FIG. 5. Proposed idea for domain decomposition: media changing on different scales.

responses on the grid that is equidistant throughout the computational domain (including the region of the absorbing boundary conditions, which are implemented as Perfectly Matched Layers (PML) [4, 5]). The elastic parameters of the materials used in the configuration are presented in Table 1 and the signals recorded on the four receivers are shown in Fig. 7—as in the previous cases, the signals recorded by the two programs are indistinguishable, with the $L^2(t)$ error approximately 0.4%. We note that to produce such an accuracy, the interface between the equidistant and the optimal regions in the nonmatching grid program had to be positioned sufficiently far from the tool, in the region where the evanescent waves, resulting from the reflections of the direct acoustic field from the tool, are minimal. The subdomain gridded equidistantly is on the left of the thin vertical line in Fig. 6 placed at

TABLE 1
Materials Used in Experiment 2

Media	Density (kg/m^3)	Compressional speed (m/s)	Shear speed (m/s)
Background formation	2120	4690	2440
Steel	7900	5800	3100
Water	1000	1500	0

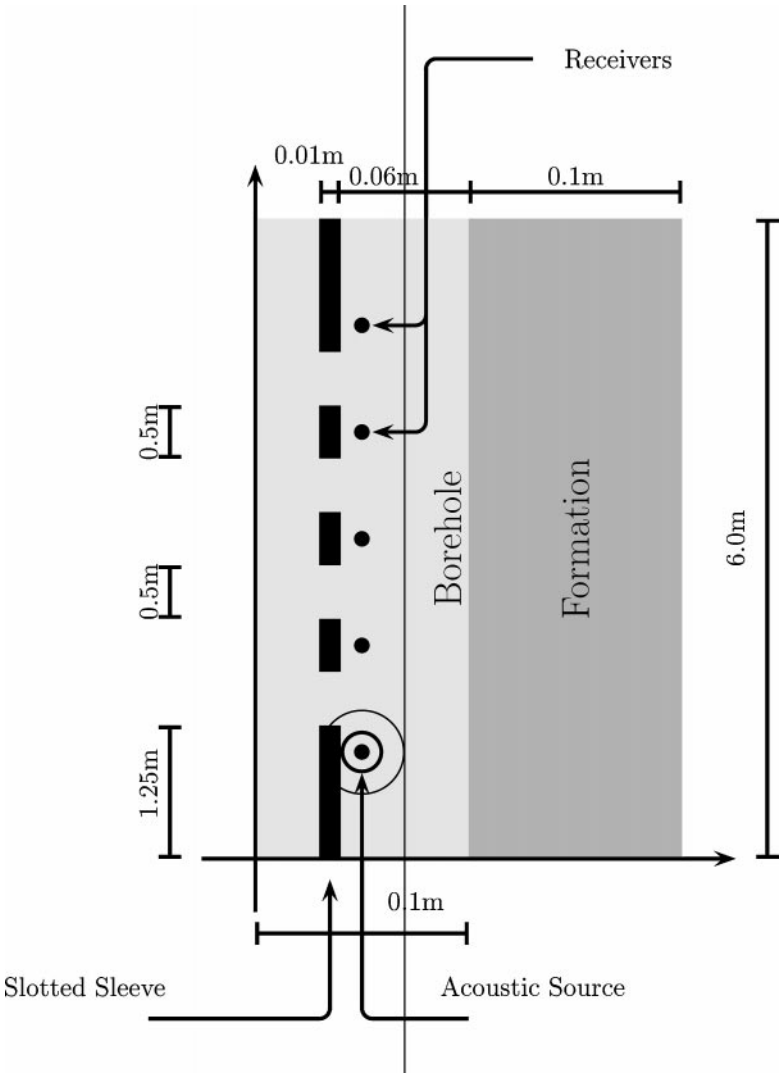

FIG. 6. Media setup for Experiment 2.

$r = 6$ cm, while the subdomain on the right of that line is gridded in the optimal fashion in the z direction.

The source signal was taken to be the first derivative of the Blackman–Harris window centered at 3.3 kHz [2]. The specturm of the source can be considered negligible around three times the center frequency; thus the minimum wavelength in the problem is 15 cm. The gridding in the r direction was kept equidistant in both subdomains and was extremely fine with 60 points per minimum wavelength, or $\Delta r = 0.25$ cm. In the axial direction the equidistant subdomain was gridded with 32 points per wavelength, while in the "optimal" region (on the right in the picture) the average number of points per wavelength was less than 4. The total number of mesh points (including the PML region) in the experiment in which the whole grid is kept equidistant was 150,000, while the total number of mesh points for the program with nonmatching grids was around 55,000. The advantage in grid points translated directly to approximately a three fold increase speed observed in real time.

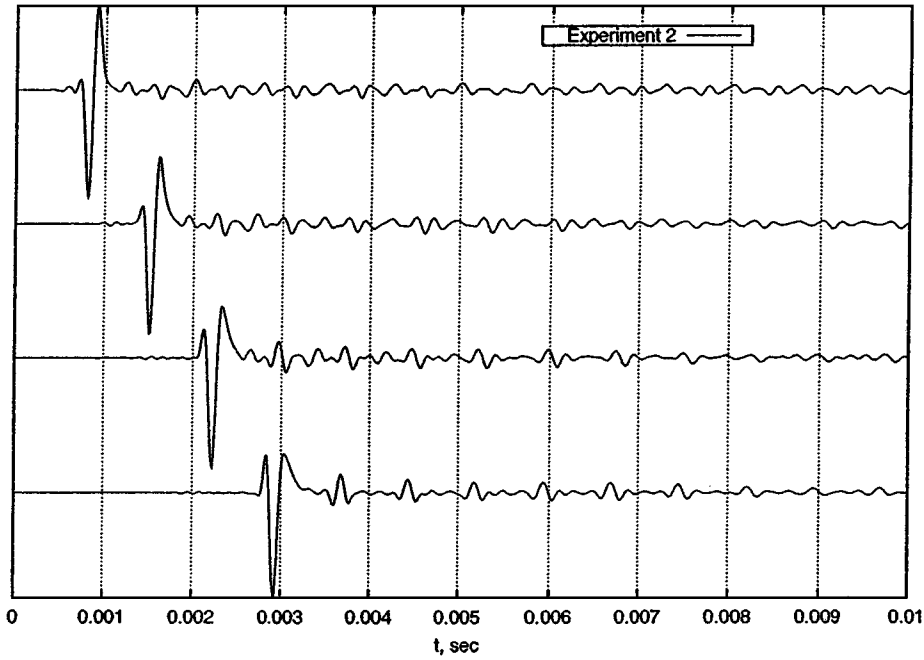

FIG. 7. Acoustic field recorded at receiver points in Experiment 2.

APPENDIX A

The Lanczos Method

Let $\mathcal{H}$ be a linear space over $\mathbb{R}$ supplied with an inner product $\langle ., . \rangle$ and complete with respect to it. Let $A : \mathcal{H} \to \mathcal{H}$ be a bounded self-adjoint linear operator and let $\varphi \in \mathcal{H}$ be a nonzero vector. The Lanczos method [13, Chap. 13] at its jth step constructs an orthonormal basis $Q_j = (\mathbf{q}_1, \ldots, \mathbf{q}_j)$ of the Krylov subspace $\mathcal{K}^j(A, \varphi) = \text{span}\{\varphi, A\varphi, \ldots, A^{j-1}\varphi\}$.

The following pseudo-Fortran code describes a Lanczos process (here $\mathbf{q}_j, \mathbf{r}, \mathbf{s} \in \mathcal{H}$ and $\alpha_j, \beta_j \in \mathbb{R}$):

$\mathbf{r} = \varphi$
$j = 1$
DO
  IF ($j = 1$) THEN; $c = 1/\|\mathbf{r}\|$; ELSE; $c = 1/\beta_{j-1}$; END IF
  $\mathbf{s} = c\mathbf{r}$
  $\mathbf{r} = A\mathbf{s}$
  IF ($j \neq 1$) $\mathbf{r} = \mathbf{r} - \beta_{j-1}\mathbf{q}_{j-1}$
  $\mathbf{q}_j = \mathbf{s}$
  $\alpha_j = \langle \mathbf{q}_j, \mathbf{r} \rangle$
  $\mathbf{r} = \mathbf{r} - \alpha_j \mathbf{q}_j$
  $\beta_j = \|\mathbf{r}\|$
  Some additional computations
  IF (*convergence*) EXIT
  $j = j + 1$
END DO

In other words, the Lanczos method performs the Gram–Schmidt orthogonalization of the vectors $\varphi, A\varphi, \ldots, A^{m-1}\varphi$ by means of the three-term recurrence

$$A\mathbf{q}_j = \beta_{j-1}\mathbf{q}_{j-1} + \alpha_j \mathbf{q}_j + \beta_j \mathbf{q}_{j+1}, \quad j = 1, 2, \ldots,$$

where $\beta_0\mathbf{q}_0$ is assumed to be 0, $\mathbf{q}_1 = \varphi/\|\varphi\|$, and $\beta_i \geq 0$.

Define by H_m the tridiagonal symmetric matrix

$$H_m = \begin{pmatrix} \alpha_1 & \beta_1 & & 0 \\ \beta_1 & \alpha_2 & \beta_2 & \vdots \\ \vdots & \ddots & \ddots & \\ 0 & \ldots & \beta_{m-1} & \alpha_m \end{pmatrix}. \tag{A.1}$$

Note that $H_m = Q_m^T A Q_m$ is the Raleigh–Ritz approximation of A on $\mathcal{K}^m(A, \varphi)$.

The exact computations in the step labeled "*Some additional computations*" depend on what we actually wish to achieve. For example, if we want to compute the eigenvalues of A, we shall find good approximants to them among those of H_m for sufficiently large m, with well separated eigenvalues converging faster than the others.

There are two fundamental identities associated with the Lanczos method. The first is the power identity

$$A^k\varphi = \|\varphi\| Q_m H_m^k \mathbf{e}_1, \quad k = 0, \ldots, m-1. \tag{A.2}$$

The Spectral Lanczos Decomposition Method (SLDM), which is based on this identity, computes the approximation for the vector $f(A)\varphi$, where f is a smooth function defined on the spectral interval of A. The SLDM approximation is given by

$$f(A)\varphi \approx \|\varphi\| Q_m f(H_m)\mathbf{e}_1. \tag{A.3}$$

Let $\tilde{T}_k$ be Chebyshev polynomials with the argument linearly shifted from the spectral interval of A on the segment $[-1, 1]$. In [9] one can find the following result:

THEOREM 1. *If the series*

$$f(x) = \sum_{k=0}^{\infty} f_k \tilde{T}_k(x) \tag{A.4}$$

converges absolutely on the spectral interval of A, then the following inequality holds:

$$\| f(A)\mathbf{q}_1 - Q_m f(H_m)\mathbf{e}_1\| \leq 2 \sum_{k=m}^{\infty} |f_k|. \tag{A.5}$$

The second identity is called the moment identity and is also sometimes referred to as the Gaussian quadrature:

$$\langle A^k\varphi, \varphi\rangle = \|\varphi\|^2 \langle H_m^k \mathbf{e}_1, \mathbf{e}_1\rangle, \qquad k = 0, \ldots, 2m-1. \tag{A.6}$$

Again, for a general enough function f we have [12]

THEOREM 2. *If the series* (A.4) *converges absolutely on the spectral interval of A, then the estimate*

$$\|\langle f(A)q_1, q_1\rangle - \langle f(H_m)e_1, e_1\rangle\| \le 2\sum_{k=2m}^{\infty} |f_k| \tag{A.7}$$

takes place.

We do not touch the problem of round-off errors in the Lanczos method, because in the programs related to this paper we use reorthogonalization, which provides us with a suitable level of stability.

There exists a relation among the Lanczos method, orthogonal polynomials, and Gaussian quadratures and moments [10].

Let μ be a unit positive measure on $\mathbb{R}$ with a finite support; it determines in the space $L_{2,\mu}$ the inner product $\langle u, v\rangle = \int uv\, d\mu$. Consider in this space the m-step Lanczos process with the operator A being the multiplication by the independent variable, i.e., $Af = xf$ for $f \in L_{2,\mu}$, and the initial vector $\varphi = 1$ (a constant unit function). The resulting Lanczos vectors π_k (with $\pi_1 = 1$) will be polynomials of degree $k-1$, orthonormal with respect to the above inner product. Moreover, the moment relation yields for $k = 0, \dots, 2m-1$

$$\int x^k\, d\mu = \langle A^k\varphi, \varphi\rangle = \|\varphi\|^2\langle H_m^k\mathbf{e}_1, \mathbf{e}_1\rangle = \sum_{i=1}^{m}\theta_i^k\mathbf{s}_{i,1}^2, \tag{A.8}$$

where $(\theta_i, \mathbf{s}_i)$ are the eigenpairs of H_m with normalized eigenvectors $\mathbf{s}_i$, and we used the eigendecomposition theorem and the fact that $\|\varphi\|^2 = \|1\|^2 = \int d\mu = 1$. This formula presents the mth-order Gaussian quadrature rule for the measure μ.

One can also define a spectral measure μ_m associated with matrix H_m which is a discrete measure whose weights are the squares of the first components of the eigenvectors of H_m positioned at the eigenvalues of H_m (the roots of π_{m+1}, which lie in the support of μ). In this case Eq. (A.8) can be rewritten as

$$\int x^k\, d\mu = \int x^k\, d\mu_m, \quad k = 0, \dots, 2m-1. \tag{A.9}$$

APPENDIX B

Computation of Grid Steps: The Stieltjes Inverse Problem

Given the impedance function of the form

$$f_m(\lambda) = \sum_{i=1}^{m}\frac{y_i}{\lambda - \theta_i}, \quad y_i > 0,\ \theta_i \le 0,\ i = 1, \dots, m, \tag{B.1}$$

we want to compute the steps of the corresponding finite-difference grid h_i and $\hat{h}_i$. This is the same as solving the inverse impedance problem for a string of k unknown point masses $\hat{h}_i$ and weightless springs with stifnesses h_i. It is known that the impedance of such a string

is a finite Stieltjes continued fraction

$$f_m(\lambda) = \cfrac{1}{\hat{h}_1\lambda + \cfrac{1}{h_1 + \cfrac{1}{\hat{h}_2\lambda + \ldots \cfrac{1}{h_{m-1} + \cfrac{1}{\hat{h}_m\lambda + \cfrac{1}{h_m}}}}}}, \tag{B.2}$$

$$h_i > 0, \quad \hat{h}_i > 0, \quad i = 1, \ldots, m, \tag{B.3}$$

i.e., we need to transform (B.1) to (B.2). Stieltjes proved that there is bijection between these two expressions, and the latter can be found with the help of the Stieltjes moment problem (sometimes also called the layer-stripping algorithm) [3, 11]. However, in some cases the classical Stieltjes method is numerically unstable. Here we present a sufficiently stable modification of this algorithm, based on the Lanczos method with reorthogonalization according to [6].

1. Compute

$$\hat{h}_1 = \frac{1}{\sum_{i=1}^m y_i}, \quad s_i = \sqrt{\hat{h}_1 y_i}, \quad i = 1, \ldots, m. \tag{B.4}$$

2. Obtain a symmetric tridiagonal matrix H_m of type (A.1), starting in the space $\mathbb{R}^m$ the Lanczos process (see Appendix A) with the matrix $\mathrm{diag}(\theta_1, \ldots, \theta_m)$ and the initial vector $(s_1, \ldots, s_m)^T$. Actually, this solves an inverse spectral problem [13, Theorem 7.2.1]. To avoid loss of orthogonality of the Lanczos vectors in finite precision arithmetic, which may cause some artificial irregularity in the grid structure, we recommend that reorthogonalization be used.

3. Perform a recursion for the grid steps,

$$h_1 = -\frac{1}{\hat{h}_1\alpha_1}, \quad \hat{h}_i = \frac{1}{\beta_{i-1}^2 h_{i-1}^2 \hat{h}_{i-1}}, \quad h_i = -\frac{1}{\alpha_i \hat{h}_i + 1/h_{i-1}}, \quad i = 2, \ldots, k,$$

starting from $\hat{h}_1$ determined in (B.4).

REFERENCES

1. M. Abramowitz and J. Stegan, *Handbook of Mathematical Functions*, Mathematics Series (Nat. Bur. of Standards, Washington, DC, 1964), Vol. 55.
2. S. Asvadurov, V. Druskin, and L. Knizhnerman, Application of the difference Gaussian rules to solution of hyperbolic problems, *J. Comput. Phys.* **158**, 116 (2000).
3. G. Baker and P. Graves-Morris, *Padé Approximants* (Addison-Wesley, London, 1996).
4. J.-P. Berenger, Perfectly matched layer for the absorbtion of electromagnetic waves, *J. Comput. Phys.* **114**, 185 (1994).
5. F. Collino and P. Monk, Optimizing the perfectly matched layer, *Comput. Metho. Appl. Mech. Eng.* **164**, 157 (1998).
6. V. Druskin and L. Knizhnerman, Gaussian spectral rules for the three-point second differences: I. A two-point positive definite problem in a semiinfinite domain, *SIAM J. Numer. Anal.* **37**, 403 (1999).

7. V. Druskin and L. Knizhnerman, Gaussian spectral rules for second order finite-differences, *Numer. Algorithms* **25**, 139 (2000).
8. V. Druskin and S. Moskow, Three-point finite difference schemes, Padé and the spectral Galerkin method: I. One-sided impedance approximation, *Math. Comput.*, in press.
9. V. L. Druskin and L. A. Knizhnerman, Two polynomial methods of calculating functions of symmetric matrices, *Comput. Math. Math. Phys.* **29**, 112 (1989).
10. G. H. Golub and G. Meurant, *Matrices, Moments and Quadrature*, Numerical Analysis Series (Longman, Sci. Tech., Harlow, 1994).
11. K. S. Kac and M. G. Krein, On the Spectral functions of the string, *Am. Math. Soc. Transl.* **103**, 19 (1974).
12. L. Knizhnerman, The simple Lanczos procedure: Estimates of the error of the Gauss quadrature formula and their applications, *Comput. Math. Math. Phys.* **36**, 1481 (1996).
13. B. Parlett, *The Symmetric Eigenvalue Problem* (Prentice-Hall/SIAM, Englewood Cliffs, NJ, 1998).
14. S. Pashkovsky, *Computational Applications of Chebyshev Polynomials and Series* (Nauka, Moscow, 1983).
15. W. Rudin, *Principles of Mathematical Analysis* (McGraw-Hill, New York, 1976).